

RESEARCH PAPER

Nanofibrillated chitosan/polycaprolactone bionanocomposite scaffold with improved tensile strength and cellular behavior

Milad Fadaie, Esmail Mirzaei *

Department of Medical Nanotechnology, School of Advanced Medical Sciences and Technologies, Shiraz University of Medical Sciences, Shiraz, Iran

ABSTRACT

Objective(s): Fabrication of scaffolds with improved mechanical properties and favorable cellular compatibility is crucial for many tissue engineering applications. This study was aimed to improve mechanical and biological properties of polycaprolactone (PCL), which is a common biocompatible and biodegradable synthetic polymer in tissue engineering. Nanofibrillated chitosan (NC) was used as a natural nanofiller to produce PCL nanobiocomposite scaffold with both enhanced mechanical properties and appropriate biological properties.

Materials and Methods: Surface morphology and orientation of chitosan nanofibrils was investigated via atomic force microscopy (AFM). PCL/NC suspension solutions with various content of NC were prepared using dimethylformamide as a dipolar solvent to obtain homogenous solutions. The scaffolds were produced through a solvent casting procedure at room temperature. The prepared scaffolds were characterized using scanning electron microscopy (SEM), attenuated total reflection- fourier transform infrared (ATR-IR) spectroscopy, X-Ray diffraction (XRD), uniaxial mechanical testing, contact angle (CA) measurements and swelling and weight loss analysis. In vitro studies were also conducted to evaluate the cellular compatibility of the prepared scaffolds.

Results: The average diameter of chitosan nanofibrils was measured 88 ± 10 nm. The existence of NC in nanocomposite was proven by ATR-FTIR and XRD results. Interestingly, incorporation of 10% of NC into PCL, improved the tensile strength of scaffolds from 2.7 to 6.5 MPa while reduced the elasticity. What is more, water contact angle of the membranes was decreased from 133° to 88° which imply more surface wettability of nanocomposite scaffolds in comparison to PCL. Furthermore, the swelling ratio and weight loss rate of bionanocomposites were increased 30% and 2.5%, respectively. MTT biocompatibility assay and cell adhesion test demonstrated superior cellular behavior of the fibroblasts on nanocomposite scaffolds in comparison to pure PCL scaffold.

Conclusion: The acquired results expressed that the PCL/NC bionanocomposite can be a reliable candidate for tissue engineering applications.

Keywords: Bionanocomposite, Nanofibrillated chitosan, Polycaprolactone, Scaffold

How to cite this article

Fadaie M, Mirzaei E. Nanofibrillated chitosan/polycaprolactone bionanocomposite scaffold with improved tensile strength and cellular behavior. *Nanomed J.* 2018; 5(2): 77-89. DOI: [10.22038/nmj.2018.005.004](https://doi.org/10.22038/nmj.2018.005.004)

INTRODUCTION

Tissue engineering is a newly emerged interdisciplinary field aims at representing novel strategies to facilitate regeneration of injured tissues as well as organs. Engineering of scaffolds with improved mechanical properties and favorable cellular compatibility is considered as an integral part of this strategy to fulfill tissue regeneration purposes [1]. Many synthetic and

natural polymers have been used for fabricating scaffolds for different tissue engineering applications [2-4]. Among them, polycaprolactone (PCL), a semi-crystalline linear FDA approved biodegradable synthetic polyester, is frequently utilized to manufacture scaffolds for many tissue engineering applications such as neural, bone, cartilage, nerve, abdominal wall, and vascular tissue engineering [5, 6]. The characteristics of PCL scaffolds should be tuned for intended tissue engineering application. PCL scaffolds with enhanced mechanical properties and appropriate

* Corresponding Author Email: e_mirzaei@sums.ac.ir

Note. This manuscript was submitted on December 29, 2017; approved on February 1, 2018

cellular compatibility is needed for many tissue engineering applications.

Chitosan is a biocompatible and biodegradable polymer fulfills a number of requirements for tissue engineering applications. This polymer is the most prominent derivate of chitin which obtained by partial N-deacetylation of the chitin [7]. Due to abundancy of chitin polymer in the nature, chitosan possesses good availability in addition to suitable reproducibility [8, 9]. Moreover, there are a number of cost-effective methods with scale up capability to supply chitosan polymer from the natural resources [10, 11]. Chitosan backbone is comprised of β -(1,4)-2-amino-2-deoxy-D-glucopyranose repeating units. The presence of hydroxyl and amino groups in chitosan structure accelerates some unique properties including biocompatibility, biodegradability, antibacterial activity, stimulation of haemostasis, and acceleration of tissue regeneration which have been investigated in a number of studies [12, 13].

The traditional microcomposite materials have been rapidly replaced by a new generation of nanostructured composites over the last two decades [14].

In definition, polymer nanocomposites are the polymeric matrices containing filler components with nanometric size (<100 nm) at least in one dimension [15]. It has been proven that, the incorporation of nano-dimension fillers into a polymeric matrix may cause dramatic improvements in physical and structural traits [16]. The enhanced physical properties of nanocomposites turn them into an appropriate choice for a wide range of biomedical [17, 18], environmental [19, 20], and industrial applications [21, 22]. Physical features of nanocomposites are not only determined by size, assembly and interfacial interactions of nanofillers but also the intrinsic properties of components. Synthetic nanomaterials like carbon nanotubes have expressed a reputable thermomechanical quality as a filler phase in a number of tissue engineering studies [23]. Nonetheless, utilization of biodegradable materials with renewable resources has been widely increased owing to growing demands emerged in research and industrial fields [17, 24]. Particularly, fabrication of green nanocomposites composed of degradable biomaterials has attracted a huge attention in the field of regenerative medicine in recent years [25, 26].

In this regard, natural nanofibrils show high aspect ratio in addition to modifiable surface-chemistry. Hence, even small proportions of natural nanofibrils derived from cellulose or chitin can develop an efficient reinforcement effect on synthetic polymers [27, 28]. Moreover, highly organized structure of these nanofibrils may influence the electrical, optical and magnetic behaviour as well as conductivity of materials [29]. There are a number of studies on reinforcing effects of embedded chitin and cellulose nanofibrils as bioactive nanofillers within PCL [30], polyurethane [31], and olylactic acid [32]. Nonetheless, inclusion of natural fillers into a hydrophobic polymer matrix can be a potentially challenging issue due to the obvious incongruity in their hydrophilicity. Surface-modification of natural nanofibrils make a better possibility for dispersion of these hydrophilic structures in more organic phases. However, it is worth mentioning that, surface chemistry of natural fillers may be altered unfavorably as a consequence of modification process [33]. In more precise word, surface functional groups such as OH, NH, and COOH which play a pivotal role in biocompatibility of materials would be hindered through the surface modification proceedings. An alternative strategy to overcome this challenge, can be employing a bipolar solvent. Fujisawa et al fabricated reinforced composites by incorporation of cellulose nanofibrils into a polystyrene matrix [34]. Using dimethylformamide (DMF) solvent in this study, resulted in homogenous dispersion of nanofillers within the polymer. Significant enhancement in mechanical behavior of the resultant nanocomposites was also the ultimate outcome.

In this study, various concentrations of chitosan nanofibril (NC) incorporated within PCL matrix in presence of DMF solvent to obtain reinforced green nanocomposites with superior bioactivity properties. The homogeneous dispersion of nanofillers in the polymeric matrix can seriously improve the interfacial interactions between two components of composite which in turn, lead to a significant enhancement in the mechanical properties of resultant composite [16]. Therefore, it is crucial to hamper the formation of NC aggregates in composite matrix as much as possible. Making a stable PCL/NC suspension was not possible without using DMF as a bipolar solvent. Solvent casting method was utilized in order to preparation of nanocomposite films. The

physicochemical properties and cellular behaviour of nanocomposites were subsequently evaluated by characterization as well as biological tests.

MATERIALS AND METHODS

Materials

The aqueous gel of chitosan nanofibrils (NC, ~2.5% w/w) was prepared by the procedure presented by (Liu, Wu, Chang, & Gao, 2011) through a top-down approach (grinding and high-pressure homogenizing) from a chitosan slurry. PCL in granular form ($M_w \sim 80000$ Da), phosphate buffered saline (powder) and glutaraldehyde (electron microscopy grade, 70%) were purchased from Sigma Aldrich (Germany). Dimethylformamide (DMF, 99.9%) and ethanol (100%) were also obtained from Merck Co.

Normal Human Dermal Fibroblast (NHDF) cells were acquired from Pasteur cell bank (Tehran, Iran). MTT ((3-(4,5-Dimethylthiazol-2-yl)-2,5-diphenyltetrazolium bromide) reagent and DMSO (cell culture grade) were purchased from Sigma Aldrich (Germany). DMEM Ham's F12 medium, Fetal Bovine Serum (FBS), penicillin and streptomycin were obtained from Gibco Invitrogen (USA).

Characterization of nanofibrils

As PCL is a thermoplastic polymer, the chitosan nanofibrils aqueous medium should be substituted by an organic phase prior to fabrication of the nanocomposite structures. Hence, a solvent-exchange step was proceeded in order to replacing the water by DMF as an organic polar solvent. After this step, purity of the solvent-exchanged chitosan nanofibrils was also measured by a weighting before and after drying.

Morphology, mean diameter size, and the orientation of solvent-exchanged chitosan nanofibrils were assessed using a Nano wizard II atomic force microscope (JPK, Germany). Prior to the microscopy, a dilute suspension of solvent exchanged NC in DMF was prepared. Then, a droplet from the suspension was deposited, smeared, and dried on a glass slide at room temperature. All scans were performed in the air and tapping mode.

Preparation of nanocomposites

Polymeric nanocomposites were prepared by solvent casting method. First, the PCL granules were dissolved in DMF at a concentration of 5% (w/w) and stirred for 2 hours at 50°C. Afterwards,

chitosan nanofibrils were added to the solution in the ratio of 2.5%, 5%, and 10% (w/w) and stirred overnight at room temperature. The samples were abbreviated as NC2.5, NC5, and NC10 correspondingly. Likewise, a pure PCL sample was provided to make a better comparison. As prepared suspensions were subsequently poured into a glass, flat-bottom, rectangular casting plates. The suspensions were casted into relatively thick films at room temperature. The casting plates were largely preserved from the dust contamination by proper covering throughout the procedure. In addition, delayed evaporation of the solvent prevented from the formation of air bubbles which may contribute to some surface defects. In the last stage, the cast films were taken out from the glass plates and stored for further investigations.

Characterization of nanocomposites scanning electron microscopy (SEM)

Scanning electron micrographs of the samples were obtained using a XL-30 scanning electron microscope (Philips, Germany). Prior to the study, samples were sputtered by an 8 nm gold-palladium layer and the surface as well as the cross-sectional morphology were investigated up to 10000x magnification.

Attenuated total reflection infrared (ATR-IR) spectroscopy

ATR-IR data of pure PCL film and a nanocomposite sample (NC10), were achieved using a Tensor 27 instrument (Bruker, USA). The acquired results were represented in the absorbance mode and in the range of 600–4,000 cm^{-1} .

Uniaxial mechanical testing

Uniaxial tensile strength of the samples was evaluated using a universal testing machine (Zwick & Roell, Germany). The sample were cut into 30×10 mm pieces and the average thickness of each strip was measured by a micrometer. The terminus part of the strips was supported with an adhesive tape and firmed to the grips The test was performed at room temperature and at the crosshead rate of 5 mm/min. The ultimate tensile strength (MPa), percentage of strain the elastic module (MPa) were acquired from the stress–strain curves. At least 5 replicate specimens were tested for each sample and the average data were graphed.

Swelling/weight loss measurement

Water absorption capacity of as prepared nanocomposites were evaluated through immersion of 20×20 mm specimens into PBS for 5, 10, 15, 20, 30, 40, 60, 90, 120 and 180 min time points. After each time points, specimens were brought out from the liquid and the surface-absorbed water was erased using a filter paper. Weight of swollen membranes was measured thereupon in order to calculating the swelling ratio:

$$\text{Weight loss(\%)} = \frac{\text{Final weight of membranes} - \text{initial weight of membranes}}{\text{initial weight of membranes}} \times 100$$

The swelling percentage values for each time point was acquired by averaging of five examinations.

Weight loss percentage of the samples was also evaluated in PBS environment at 25°C. Sample were cut into 30×30 mm pieces, weighted and submerged in PBS for 1, 2, 3, 5, 7, and 14 days. The specimens then expelled from the PBS and dried out in the open air. Following this, specimens weighted precisely and the weight loss ratio acquired from the following equation:

$$\text{Weight loss(\%)} = \frac{\text{Final weight of membranes} - \text{initial weight of membranes}}{\text{initial weight of membranes}} \times 100$$

Each calculated weight loss result was the average value of five repeated test.

X-Ray diffraction (XRD)

XRD patterns were collected using a PW 1710 diffractometer (Philips, The Netherlands) for chosen samples (PCL and NC10). The pattern recording was carried out by the Cu/K α irradiations ($\lambda = 0.1541$ nm), scan speed of 2° min⁻¹ and 2-theta range of 5-70°.

Contact angle (CA) measurement

Static contact angle measurements were carried out by using an OCA 15 plus contact angle meter (Dataphysics, Germany) at ambient temperature. Water droplets with determined volume were utilized for the experiments and the data were recorded using a high speed framing camera within 20 seconds after water-scaffold contact in the precision of $\pm 0.1^\circ$. At least 5 separate recordings were averaged and reported for each type of sample.

In-vitro studies

NHDF cells were cultured in DMEM-F12 enriched with 10% FBS and 1% antibiotics (penicillin-streptomycin) and passaged

approximately every 2 days (80% confluency). Circular discs of the scaffolds were prepared in diameter of ~5 mm prior to the in-vitro tests. The specimens were pasted at the bottom of a 96-well cell culture plate by means of dilute agarose gel (n=4). After this, the membranes were disinfected by immersion in ethanol (70% v/v) for 15min and rinsing by PBS three times for 5 min. following that dried scaffolds were sterilized under UV-irradiation for 30 min. NHDF cells were subsequently seeded on the surface of scaffolds at a cell density of 1×10^4 cells and flooded with supplemented culture medium in total volume of 400 μ l. The cell-scaffolds were incubated at standard culture conditions (37°C and 5% CO₂) for defined time intervals.

MTT proliferation assay

Evaluation of cell viability through the MTT assay is based on the mechanism of reducing tetrazolium salt to formazan via mitochondrial activity of the viable cells. Hereupon, the level of tetrazolium reduction may quantitatively indicate the rate of metabolically-active cells. Cell proliferation of cultured cells on the scaffolds were performed by MTT assay at 24h, 48h, and 72h time points. After each time interval, cell supernatants were extracted and the scaffolds washed by PBS three times. Thereafter, 100 μ l of MTT solution (2.5% w/v in fresh media) was added to each well and four hours incubated at 37 °C in humidified atmosphere. Next, the solution was removed, 100 μ l of DMSO was added to in order to solubilizing the formed formazan crystals. The optical density (OD) of each well at wavelength of 570 nm was measured by a Polar star omega microplate reader (BMG LABTECH, Germany). Finally, the viability percentage of each group was calculated using the following equation:

$$\text{Cell Viability (\%)} = \frac{\text{Mean OD of the test group}}{\text{Mean OD of the control}} \times 100$$

Cell attachment study

Attachment of the cultured cells on scaffold was studied 12h post cell-seeding. Briefly, supernatant of the scaffolds was removed after 12h and the cell-scaffolds were gently rinsed by PBS three times. Afterwards the cultured NHDFs were fixed with glutaraldehyde (electron microscopy grade, 2.5% v/v) for 1h at room temperature. Next, fixing solution was removed and any trace of glutaraldehyde was wiped out from cell-seeded

membranes through slight rinsing by PBS. The fixation process was followed by sequential dehydration in 10%, 30%, 50%, 70%, 90%, and 100% ethanol and air-dried overnight. The cell-containing scaffolds were coated with a thin gold/palladium layer and analyzed by a TESCAN-Vega 3 SEM (Czech Republic).

Statistical Analysis

The acquired data in this study achieved from at least five independent examinations and expressed in mean \pm SD and. The obtained values statistically analyzed using a one-way ANOVA test and then Tukey Post Hoc analysis was performed to make comparisons between various groups. Prism7 program was employed for the statistical analyses and the difference between groups considered significant if $p < 0.05$.

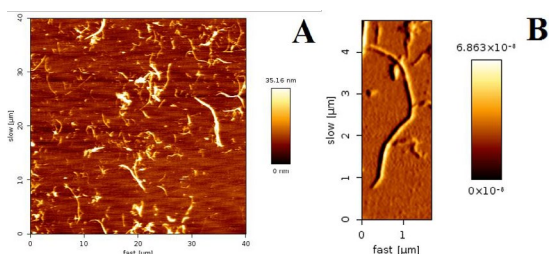


Fig 1. AFM image of (a) chitosan nanofibrils (b) an individual chitosan nanofibril

RESULTS AND DISCUSSION

Morphology of Nanofibrils

Fig 1. shows atomic force micrographs of solvent-exchanged chitosan nanofibrils. As can be seen, the fibrillar morphology of solvent-exchanged nanofibrils was preserved to a large extent. However, there was some distinguishable aggregations which presumed to be in association with the sample preparation step. It was interestingly realized that, chitosan nanofibrils have a strong tendency to be adhered together and form nanofibrillar aggregates while drying. This can be in correlation with Abdul Khalil et al finding about the adverse morphological effects of drying process on unique properties of cellulose nanofibrils [24]. Hereupon, solvent-exchange was considered as the preferred method in our study. In addition, mean diameter of the chitosan nanofibrils was evaluated by measuring merely individual fibrils without inclusion of aggregations ($n=50$). The calculated average fibrils diameter was 88 ± 10 nm which was an indicative of their nanoscale feature.

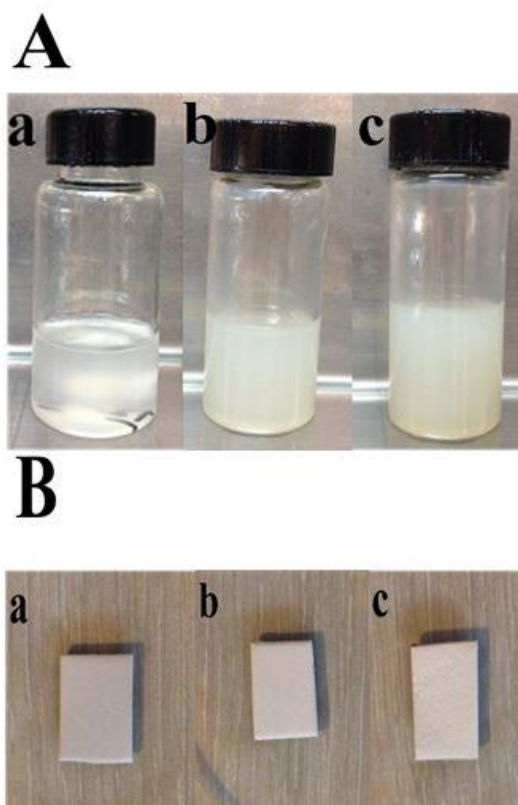


Fig 2. (A) As prepared (a) PCL, (b) NC5, (c) NC10 suspensions (B) Macroscopic (gross) projection of (a) PCL, (b) NC5, (c) NC10 solvent cast nanocomposite films

Morphological Properties of Nanocomposites

As can be seen in Fig 2A, a stable and homogeneous suspension of PCL/NC was obtained even in the highest concentration of embedded nanofillers. Moreover, in a gross observation, nanocomposite films largely resembled to the pure PCL film (Fig 2B).

Fig 3. is representative for scanning electron micrographs of solvent cast films. As can be observed, neat PCL films indicated a fractured surface morphology with relatively large pores in dimension of $10-30\mu\text{m}$ (Fig 3A). Increasing concentration of chitosan nanofibrils incorporated in PCL matrix, led to a moderate decrement in proportion of fractures as well as pore size. However, no sign of fillers aggregation or formation of PCL globules could be distinguished on the surface of nanocomposite films (Fig 3B-D). It was not only attributed to homogeneous distribution of nanofillers within the polymeric matrix, but also appropriate interfacial interactions between the two phases [18, 35].

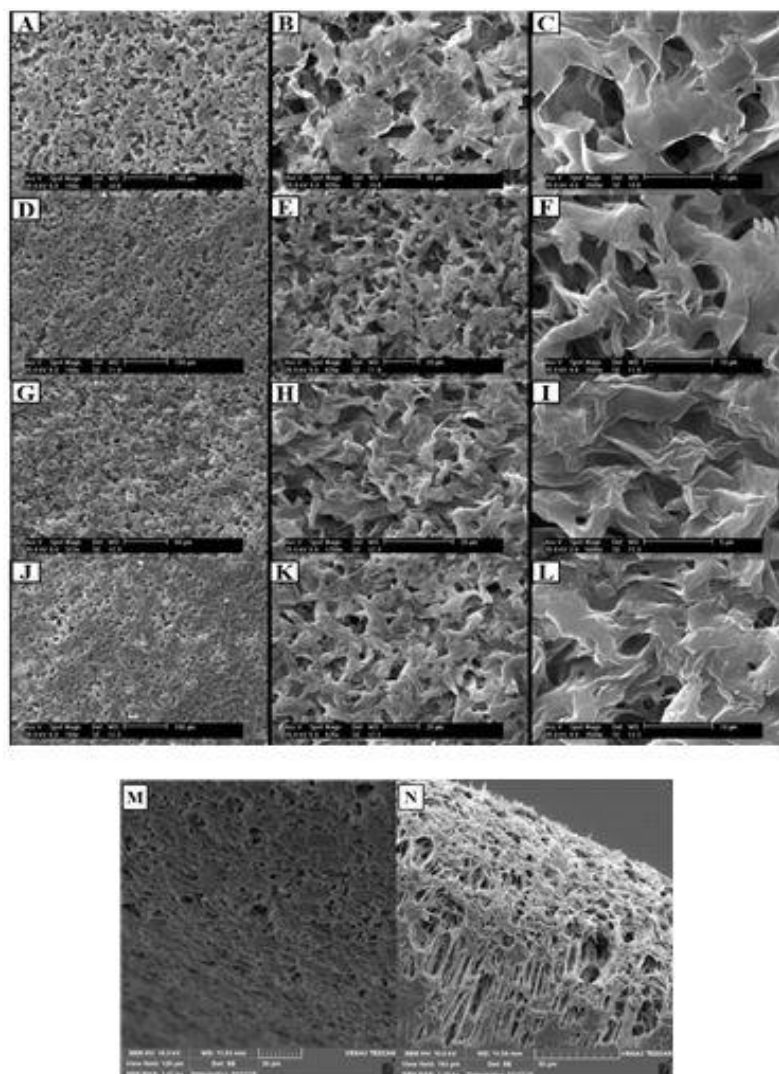


Fig 3. Scanning electron micrographs of pure PCL (A-C), and PCL nanofibrillated chitosan nanocomposites, NC2.5 (D-F), NC5 (G-I), NC10 (J-L), in different magnifications. M and N are representative for cross-sectional micrographs of NC5 sample

In addition, solids content of suspensions remained constant throughout the study in order to investigating the morphological effects of including nanofillers specifically. Superior uniformity of nanocomposite surfaces and decreased number of pores can improve the mechanical properties of scaffolds. Although a slight hindrance in surface roughness of nanocomposites may diminish wettability of the scaffolds, inclusion of a hydrophilic nanofillers can be a rectifying factor to this drawback. The obtained cross-sectional micrographs of NC5 sample (Fig 3E) clearly confirmed the presence of an interconnected network of pores in nanocomposite structure. It is

expected that, the interconnectivity of pores cell infiltration into the depth of scaffolds [18].

ATR-FTIR analysis

ATR-FTIR spectrum of PCL and PCL/NC composite is presented in Fig 4. Pure PCL film exhibits an intense peak at 1721 cm^{-1} which is the characteristic peak of PCL and assigned to the carbonyl stretching [36]. This peak weakened in nanocomposite spectrum suggesting reduced content of PCL. However, 1578 , 1647 , and 3371 cm^{-1} bands are also distinguishable in nanocomposite which ascribed to NH bending of amide II, carbonyl stretching of amide I, and NH

stretching of the free amino groups in chitosan correspondingly [37]. Nonetheless, the intensity of these peaks was not considerable due to the small proportion of embedded NC. The interpretation of ATR-FTIR results confirmed the successful incorporation of chitosan nanofibrils into the PCL matrix. As well as this, presence of NH groups on the surface of nanocomposite structures was affirmable through the ATR-FTIR analysis which could be advantageous for a number of tissue engineering applications.

Mechanical properties

Analyzing of stress-strain curves gives us beneficial information about the mechanical properties of scaffolds. As illustrated in Fig 5, ultimate tensile strength of nanocomposites experiences an increasing trend by augmenting in amount of the nanofiller.

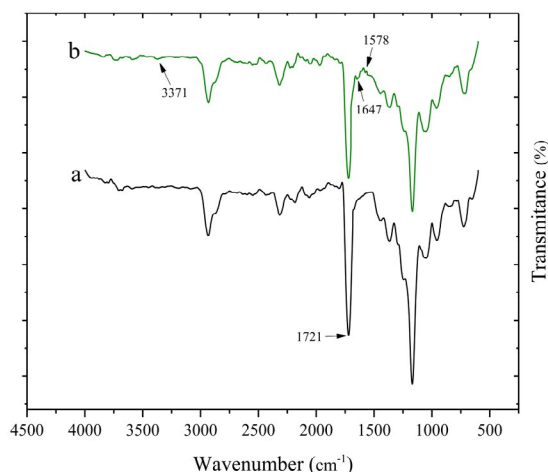


Fig 4. ATR-FTIR spectrum of (a) PCL and (b) NC10 sample. The arrows indicate the wavenumber of characteristic peaks for PCL (1721 cm⁻¹) and NC (1578, 1647, and 3371 cm⁻¹)

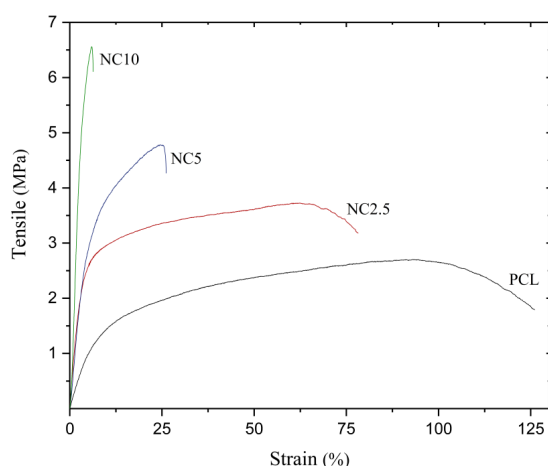


Fig 5. Stress-strain curves of PCL and NC composite samples

Stress-strain curves show a 260% increase in tensile strength of NC10 sample (6.5MPa) compared to pure PCL (2.7 MPa). Rigidity and uniform distribution of embedded nanofillers as well as PCL/NC strong interfacial interactions can be the contributing factors to this increment [38, 39]. In addition, incorporating the higher amount of chitosan nanofibrils into the PCL matrix resulted in fabrication of less porous nanocomposites as discussed in SEM section. Hindrance of porosity in architecture of scaffolds can make a considerable reinforcing effect on the mechanical behaviour as well [40, 41]. It is worth noting that, balancing of porosity is a critical factor due to its vital role in cellular compatibility of scaffolds [42]. The mechanical parameters of membranes have been also categorized in Table 1. From the table, the elastic module of PCL sample increased over 18-folded through introducing of 10% NC. However, elongation of nanocomposite films reduced dramatically in the same time. It can be due to the fact that, small amount of chitosan nanofibrils can intensify the scaffold stiffness and brittleness simultaneously. From this, inclusion of NC within PCL polymer enhances the tensile and elastic module in expense of decreased elongation. These results are largely in agreement with the literature [43, 44].

XRD study

Fig 6 represents the XRD analyses of neat PCL and NC10 sample. As is illustrated, PCL showed two sharp peaks at $2\theta = 21.5^\circ$ and 23.85° which are assigned to (1 1 0) and (2 0 0) diffraction planes respectively [45]. Moreover, there is a relatively weak peak positioned at $2\theta = 15.7^\circ$. These peaks are characteristic of PCL polymer and indicative for its semi-crystalline nature[46, 47]. In terms of NC10 diffractogram, typical peaks of PCL showed a moderate reduction.

Table 1. Summeryed mechanical parameters obtained from tensile strength analysis of the samples

Sample	Elastic module (MPa)	UTS (MPa)	Stain (%)
PCL	10	2.7	125
NC2.5	22	3.72	78
NC5	31	4.76	26.1
NC10	184	6.5	6.3

*UTS: Ultimate Tensile Strength

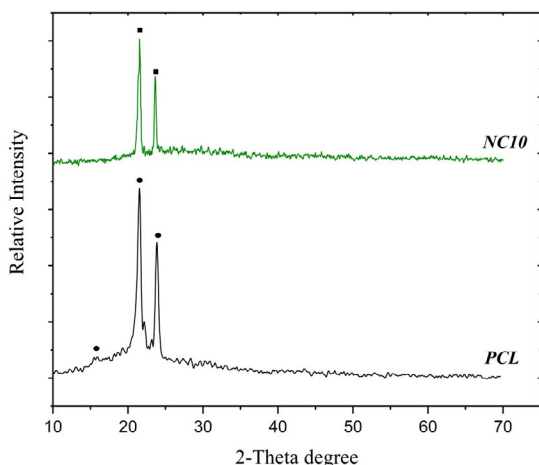


Fig 6. XRD patterns of PCL and NC10 samples. The signs show the characteristic peaks concerning each sample

It can be owing to decreased crystallinity of nanocomposite as a result of introducing chitosan nanofibrils. Lower amount of PCL in nanocomposite structure can be another potential reason for this phenomenon. Additionally, a slight shift ($\sim 0.2^\circ$) in the position of intense peaks could be detected in nanocomposite XRD pattern. Nonetheless, there was no distinguishable sign of chitosan peaks in nanocomposite sample due to the small proportion of incorporated chitosan polymer [48]. It is expected that, reduced crystallinity of the nanocomposite scaffolds leads accelerated degradation structures [49].

Surface wettability

Water contact angle measurement was carried out in order to assessing the hydrophilicity alterations in nanocomposite scaffolds. As presented in Fig 7, pure PCL film exhibits poor hydrophilicity with an average contact angle of 131.4° which is in line with hydrophobic nature of the polymer [50]. The contact angle value of PCL reduced to 98.9° , 91° , and 88.5° through the addition of 2.5%, 5%, and 10% of NC correspondingly.

Incorporation of chitosan within the PCL matrix may present a number of hydrophilic groups such as NH and OH on the surface nanocomposite membranes [51]. These functional groups possess a considerable capability to absorb great amount of water molecules.

Therefore, wettability of PCL scaffold can be seriously modified by addition of chitosan nanofibrils indeed. As well as this, decreased surface roughness of nanocomposite films plays a crucial role in reduction of wettability [52]. High interfacial surface between the scaffold and water droplet can cause a significant decrement in contact angle. More precisely, scaffolds with less fractured surfaces demonstrate improved hydrophilicity.

From this, superior wettability of PCL/NC nanocomposite scaffolds can be also explained by their smoother morphology in comparison with pure PCL.

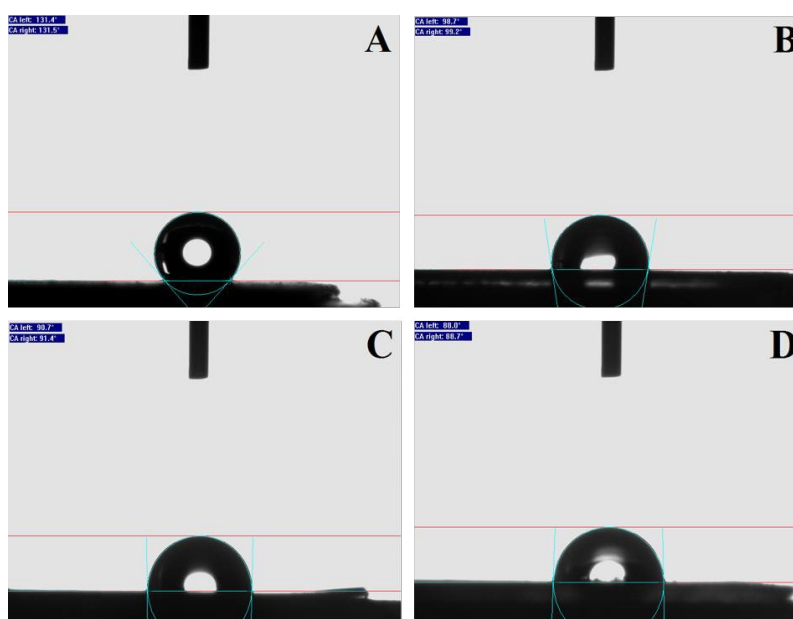


Fig 7. Contact angle measurement for PCL (A), NC2.5 (B), NC5 (C), and NC10 (D) samples

Swelling ratio

Fig 8A represents swelling behaviour of pure PCL and NC10 nanocomposite samples in PBS environment in a six-hour incubation period. In general, PCL polymer scaffolds exhibit inferior water uptake capacity due to their hydrophobic nature [53].

However, porosity of structures can be another key factor in acceleration of water permeation into the depth of structure [54]. As illustrated in the graph, capability of PCL film to absorb water was about 10% of its initial weight. Interestingly, incorporating 10% of chitosan nanofibrils led to a significant increase in amount of uptaken water up to 42%.

There are couple of explanation for improving in swelling ratio of nanocomposite scaffold. It may be attributed to modification of PCL surface hydrophobicity which accelerates surface absorption of water molecules. As well as this, embedded chitosan nanofibrils not only are able to create a hydrophilic pathway within the PCL matrix but also increase amorphous characteristic of structure in order to enhancing penetration of water into the depth of scaffolds. It is worth mentioning that, interconnected network of pores presented in the architecture of samples can be an intensifying factor in swelling of scaffolds [43]. These finding are largely in accordance with previous similar studies [55].

Weight loss rate

The extent of weight loss for PCL and NC10 samples has been evaluated over 12 weeks and graphed in Fig 8B.

As a general trend, PCL sample lost approximately 2% of the initial weight over 12 weeks, however, the weight loss for NC10 sample was about 4.5% in the same period. Molecular weight of PCL seriously affects its degradation kinetic [56]. PCL with high molecular weight possess longer polymer chains with numerous ester linkages to be cleaved which makes the degradation rate slower [57]. Additionally, diminishing in PCL crystallinity may have diminishing effect on degradability of polymer [58]. Although molecular weight of PCL did not alter in the scaffolds, nanocomposite samples showed lower crystallinity compared to pure PCL. Degradation process of PCL polymer is mostly based on enzymatic degradation and/or non-enzymatic hydrolysis [59]. Sterilized PBS was used in the weight loss experiment so as to reducing the enzymatic degradation of PCL as much as possible. However, it is presumed that; pure PCL films are commonly undertaken superficial erosion due to the inferior penetration of water molecules into the scaffold [6]. On the contrary, nanocomposite samples show superior water absorption which is contributing factor to acceleration of non-enzymatic hydrolysis. From the acquired results, blending of PCL polymer with chitosan nanofibrils can merely enhance the non-enzymatic hydrolysis process. Relative hindrance of PCL enzymatic degradation through combining with chitosan has been also proven in previous studies [60]. As PCL/NC structures are less susceptible to bacterial degradation, these structures can be potentially utilized in a number of biomedical applications specifically for medical implants and tissue engineering scaffolds.

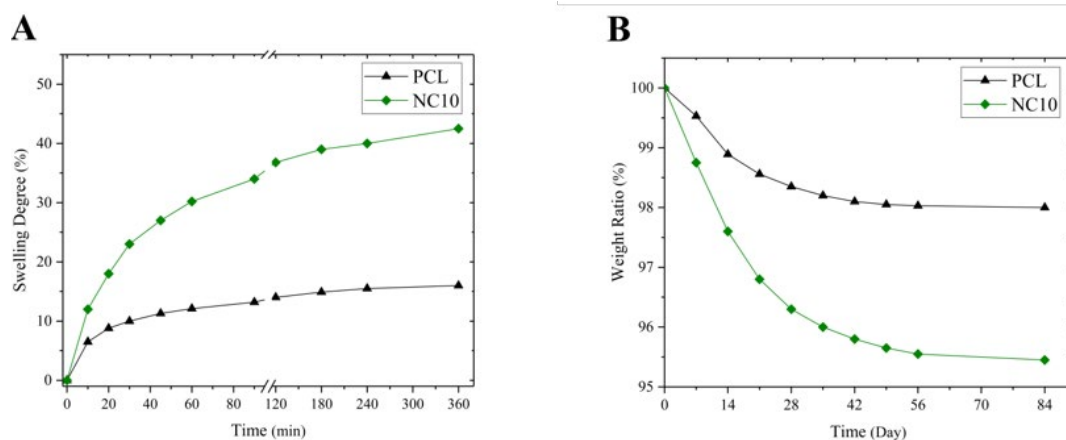


Fig 8. Swelling degree (A) and weight loss ratio (B) graphs related to PCL and NC10 sample

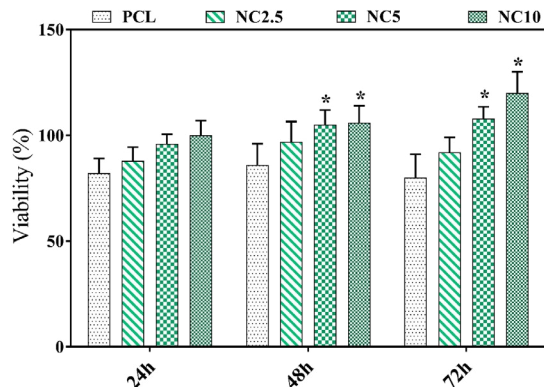


Fig 9. MTT proliferation assay results at 24, 48, and 72 hours time-points. * sign exhibits statically significant difference of the NC5 and NC10 groups with PCL ($P < 0.05$)

Cellular behaviour

Fig 9 depicts the quantified viability of NHDF cells cultured on the PCL and PCL/NC scaffolds in 24, 48, and 72h time intervals.

Although, viability of PCL sample was inferior to nanocomposite values, there was not a statistically significant difference between the viability of groups in the first 24 hours.

However, NC5 and NC10 cell-containing samples were more metabolically-active at day 2 and 3 comparing with pure PCL membrane ($P < 0.05$). The highest cell proliferation belonged to the nanocomposite scaffolds with 10% of NC.

These viability results can be explained by higher hydrophobicity of PCL scaffold as well as increased number of reactive sites on the surface of nanocomposites [43]. Even though synthetic polymers represent superior mechanical properties, cellular compatibility of these structures is not desirable in the most cases. The cytocompatibility of materials is largely hinges on three major factors including composition, surface chemistry and the morphological traits [61]. Hydrophobic nature of PCL hinders the cellular interactions [62] which not only limits primary adhesion of the cultured cells but also cell spreading, cell infiltration, and cell proliferation. PCL/NC scaffolds exhibited a considerable improvement in surface wettability as mentioned in previous section. In addition, NC composites possess a modified and more bioactive surface chemistry in comparison with bare PCL structure due to the cationic properties of chitosan nanofibrils.

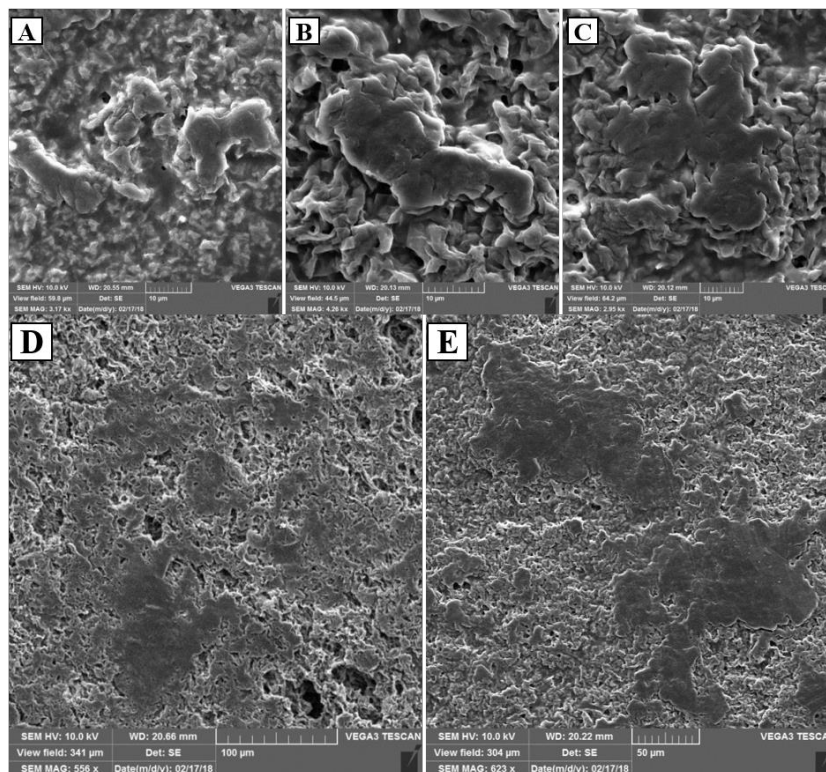


Fig 10. SEM projections of adhered cells on the scaffolds: (A) PCL, (B) NC5, (C) NC10 after 12h of incubation. D and E respectively show NC5 and NC10 cell-containing scaffolds in lower magnifications which Cell-mass regions are clearly distinguishable

Accordingly, cellular compatibility of the nanocomposite samples can be enhanced in presence of positively-charged amino groups on the surface [63].

More precisely, negative net charge of cell membrane proteins facilitates the potential interactions between seeded cells and NC containing scaffolds.

Cell adhesion of PCL membrane and NC-embedded nanocomposites was evaluated by SEM observation. Fig 10 demonstrates scanning electron micrographs of the attached cells on different samples after 12h of incubation. According to SEM images with higher magnifications (Fig 10A-C), the cultured cells on NC5 and NC10 sample showed spreading morphology with remarkable elongation in x-y axis. In contrast, fibroblast cultured on neat PCL scaffold have a relatively round morphology without any significant extension. Higher roughness of the surface can be a critical factor in improving the attachment as well as spreading of the cultured cells [64]. Although pure PCL scaffold shows higher surface roughness, the adhesion cell on this sample was considerably hindered. Therefore, modified surface hydrophilicity of the nanocomposites can be the underlying reason for enhanced cell-adhering and cell-spreading on these samples [65, 66]. Some integrated cell masses are also distinguishable in Fig 10 D, E spread throughout the surface of the nanocomposite scaffolds. It is thought that these structures were formed owing to fast duplication rate of NHDFs in addition to presence of good substrate to promote cell growth.

CONCLUSION

Neat PCL, and PCL nanobiocomposite scaffolds with various amount of nanofibrillated chitosan were successfully fabricated through solvent cast method. The purpose of the research was to produce PCL nanocomposite scaffolds with improved mechanical properties and proper cellular compatibility. This results demonstrates that incorporation of chitosan nanofibrils within PCL can make a considerable reinforcing effect on mechanical integrity of the structures in addition to serious morphological alterations. As well as this, presence of chitosan on the surface and into the matrix of PCL was confirmed via ATR-FTIR and XRD analysis. The embedding of chitosan nanofibrils favorably influences the surface wettability, swelling ratio and weight loss percentage of PCL

membranes. Regarding cytocompatibility, inclusion of NC improves the cell viability, adhesion, and spreading to a large extent. As-prepared PCL/NC nanocomposites can be considered as potentially biocompatible scaffolds for utilization in various tissue engineering applications.

ACKNOWLEDGEMENTS

This project was part of a Master of Science thesis in medical nanotechnology and financially supported by Shiraz University of Medical Sciences (SUMS), Shiraz, Iran. (Grant No. 12374-74-01- 95).

REFERENCES

1. Lanza R, Langer R, Vacanti JP. Principles of Tissue Engineering (Fourth Edition). Boston: Academic Press; 2014.
2. Armentano I, Dottori M, Fortunati E, Mattioli S, Kenny JM. Biodegradable polymer matrix nanocomposites for tissue engineering: A review. *Polym Degrad Stab.* 2010; 95(11): 2126-2146
3. Martina M, Hutmacher DW. Biodegradable polymers applied in tissue engineering research: a review. *Polym Int.* 2007; 56(2): 145-157.
4. Faghihi F, Mirzaei E, Sarveazad A, Ai J, Ebrahimi Barough S, Lotfi A, Joghataei MT. Differentiation Potential of Human Bone Marrow Mesenchymal Stem Cells into Motorneuron-like Cells on Electrospun Gelatin Membrane. *J Mol Neurosci.* 2015; 55(4): 845-853.
5. Asvar Z, Mirzaei E, Azarpira N, Geramizadeh B, Fadaie M. Evaluation of electrospinning parameters on the tensile strength and suture retention strength of polycaprolactone nanofibrous scaffolds through surface response methodology. *J Mech Behav Biomed Mater.* 2017; 75: 369-378.
6. Abedalwafa M, Wang F, Wang L, Li C. Biodegradable poly-epsilon-caprolactone (PCL) for tissue engineering applications: a review. *Rev Adv Mater Sci.* 2013; 34(2): 123-140.
7. Kumar MNR. A review of chitin and chitosan applications. *React Funct Polym.* 2000; 46(1): 1-27.
8. Ravi Kumar MNV. A review of chitin and chitosan applications. *React Funct Polym.* 2000; 46(1): 1-27.
9. Yu L, Dean K, Li L. Polymer blends and composites from renewable resources. *Prog Polym Sci.* 2006; 31(6): 576-602.
10. Hayes M, Carney B, Slater J, Brück W. Mining marine shellfish wastes for bioactive molecules: Chitin and chitosan ndash; Part A: extraction methods. *Biotechnol J.* 2008; 3(7): 871-877.
11. Kaur S, Dhillon GS. The versatile biopolymer chitosan: potential sources, evaluation of extraction methods and applications. *Crit Rev Microbiol.* 2014; 40(2): 155-175.
12. Chatelet C, Damour O, Domard A. Influence of the degree of acetylation on some biological properties of chitosan films. *Biomaterials.* 2001; 22(3): 261-268.
13. Rinaudo M. Chitin and chitosan: properties and applications. *Prog Polym Sci.* 2006; 31(7): 603-632.
14. Siqueira G, Bras J, Follain N, Belbekhouche S, Marais S, Dufresne A. Thermal and mechanical properties of bionanocomposites reinforced by Luffa cylindrica cellulose nanocrystals. *Carbohydr Polym.* 2013; 91(2): 711-717.

15. Oksman K, Mathew AP, Bondeson D, Kvien I. Manufacturing process of cellulose whiskers/poly(lactic acid) nanocomposites. *Composites Sci Technol*. 2006; 66(15): 2776-2784.
16. Saba N, Tahir PM, Jawaid M. A review on potentiality of nano filler/natural fiber filled polymer hybrid composites. *Polymers*. 2014; 6(8): 2247-2273.
17. Siqueira G, Bras J, Dufresne A. Cellulosic bionanocomposites: a review of preparation, properties and applications. *Polymers*. 2010; 2(4): 728-7265.
18. Liu M, Zheng H, Chen J, Li S, Huang J, Zhou C. Chitosan-chitin nanocrystal composite scaffolds for tissue engineering. *Carbohydr Polym*. 2016; 152: 832-840.
19. Zhu J, Wang Y, Liu J, Zhang Y. Facile one-pot synthesis of novel spherical zeolite-reduced graphene oxide composites for cationic dye adsorption. *Ind Eng Chem Res*. 2014; 53(35): 13711-13717.
20. Yang Y, Xie Y, Pang L, Li M, Song X, Wen J, Zhao H. Preparation of reduced graphene oxide/poly (acrylamide) nanocomposite and its adsorption of Pb (II) and methylene blue. *Langmuir*. 2013; 29(34): 10727-10736.
21. Mi H-Y, Jing X, Peng J, Salick MR, Peng X-F, Turng L-S. Poly (ϵ -caprolactone) (PCL)/cellulose nano-crystal (CNC) nanocomposites and foams. *Cellulose*. 2014; 21(4): 2727-2741.
22. Durango A, Soares N, Andrade N. Microbiological evaluation of an edible antimicrobial coating on minimally processed carrots. *Food Control*. 2006; 17(5): 336-341.
23. Harrison BS, Atala A. Carbon nanotube applications for tissue engineering. *Biomaterials*. 2007; 28(2): 344-353.
24. Khalil HPSA, Davoudpour Y, Aprilia NAS, Mustapha A, Hossain S, Islam N, Dungani R. Nanocellulose-Based Polymer Nanocomposite: Isolation, Characterization and Applications. *Nanocellulose Polymer Nanocomposites*: John Wiley & Sons, Inc.; 2014. p. 273-309.
25. Darder M, Aranda P, Ruiz-Hitzky E. Bionanocomposites: a new concept of ecological, bioinspired, and functional hybrid materials. *Adv Mater*. 2007; 19(10): 1309-1319.
26. Biswas A, Bayer IS, Zhao H, Wang T, Watanabe F, Biris AS. Design and synthesis of biomimetic multicomponent all-bone-minerals bionanocomposites. *Biomacromolecules*. 2010; 11(10): 2545-2549.
27. Siqueira G, Bras J, Dufresne A. Cellulose whiskers versus microfibrils: influence of the nature of the nanoparticle and its surface functionalization on the thermal and mechanical properties of nanocomposites. *Biomacromolecules*. 2008; 10(2): 425-432.
28. Chen B, Sun K, Ren T. Mechanical and viscoelastic properties of chitin fiber reinforced poly (ϵ -caprolactone). *Eur Polym J*. 2005; 41(3): 453-457.
29. Cherian BM, Leão AL, de Souza SF, Costa LMM, de Olyveira GM, Kottaisamy M, Nagarajan E, Thomas S. Cellulose nanocomposites with nanofibres isolated from pineapple leaf fibers for medical applications. *Carbohydr Polym*. 2011; 86(4): 1790-1798.
30. Lin N, Chen G, Huang J, Dufresne A, Chang PR. Effects of polymer-grafted natural nanocrystals on the structure and mechanical properties of poly (lactic acid): A case of cellulose whisker-graft-polycaprolactone. *J Appl Polym Sci*. 2009; 113(5): 3417-3425.
31. Juntaro J, Ummartyotin S, Sain M, Manuspiya H. Bacterial cellulose reinforced polyurethane-based resin nanocomposite: a study of how ethanol and processing pressure affect physical, mechanical and dielectric properties. *Carbohydr Polym*. 2012; 87(4): 2464-2469.
32. Xiang C, Taylor AG, Hinestroza JP, Frey MW. Controlled release of nonionic compounds from poly (lactic acid)/cellulose nanocrystal nanocomposite fibers. *J Appl Polym Sci*. 2013; 127(1): 79-86.
33. Ji Y-l, Wolfe PS, Rodriguez IA, Bowlin GL. Preparation of chitin nanofibril/polycaprolactone nanocomposite from a nonaqueous medium suspension. *Carbohydr Polym*. 2012; 87(3): 2313-2319.
34. Fujisawa S, Saito T, Kimura S, Iwata T, Isogai A. Comparison of mechanical reinforcement effects of surface-modified cellulose nanofibrils and carbon nanotubes in PLLA composites. *Composites Sci Technol*. 2014; 90: 96-101.
35. Kiziltas A, Nazari B, Kiziltas EE, Gardner DJ, Han Y, Rushing TS. Cellulose NANOFIBER-polyethylene nanocomposites modified by polyvinyl alcohol. *J Appl Polym Sci*. 2016; 133(6): 42933- 42933.
36. Gomes S, Rodrigues G, Martins G, Roberto M, Mafra M, Henriques C, Silva J. In vitro and in vivo evaluation of electrospun nanofibers of PCL, chitosan and gelatin: a comparative study. *Mater Sci Eng C*. 2015; 46: 348-358.
37. Ghorbani FM, Kaffashi B, Shokrollahi P, Seyedjafari E, Ardeshiryajimi A. PCL/chitosan/Zn-doped nHA electrospun nanocomposite scaffold promotes adipose derived stem cells adhesion and proliferation. *Carbohydr Polym*. 2015; 118: 133-142.
38. Cao X, Dong H, Li CM. New nanocomposite materials reinforced with flax cellulose nanocrystals in waterborne polyurethane. *Biomacromolecules*. 2007; 8(3): 899-904.
39. Sarasam A, Madihally SV. Characterization of chitosan-polycaprolactone blends for tissue engineering applications. *Biomaterials*. 2005; 26(27): 5500-5508.
40. Liu M, Dai L, Shi H, Xiong S, Zhou C. In vitro evaluation of alginate/halloysite nanotube composite scaffolds for tissue engineering. *Mater Sci Eng C*. 2015; 49: 700-712.
41. Venkatesan J, Qian Z-J, Ryu B, Kumar NA, Kim S-K. Preparation and characterization of carbon nanotube-grafted-chitosan-natural hydroxyapatite composite for bone tissue engineering. *Carbohydr Polym*. 2011; 83(2): 569-577.
42. Ikeda R, Fujioka H, Nagura I, Kokubu T, Toyokawa N, Inui A, Makino T, Kaneko H, Doita M, Kurosaka M. The effect of porosity and mechanical property of a synthetic polymer scaffold on repair of osteochondral defects. *Int Orthop*. 2009; 33(3): 821-828.
43. Surucu S, Sasmazel HT. Development of core-shell coaxially electrospun composite PCL/chitosan scaffolds. *Int J Biol Macromol*. 2016; 92: 321-328.
44. Van der Schueren L, Steyaert I, De Schoenmaker B, De Clerck K. Polycaprolactone/chitosan blend nanofibres electrospun from an acetic acid/formic acid solvent system. *Carbohydr Polym*. 2012; 88(4): 1221-1226.
45. Bras J, Hassan ML, Bruzesse C, Hassan EA, El-Wakil NA, Dufresne A. Mechanical, barrier, and biodegradability properties of bagasse cellulose whiskers reinforced natural rubber nanocomposites. *Ind Crops Prod*. 2010; 32(3): 627-633.
46. Raucci M, D'Antò V, Guarino V, Sardella E, Zeppetelli S, Favia P, Ambrosio L. Biomaterialized porous composite scaffolds prepared by chemical synthesis for bone tissue regeneration. *Acta Biomater*. 2010; 6(10): 4090-4099.
47. Fabbri P, Bondioli F, Messori M, Bartoli C, Dinucci D,

- Chiellini F. Porous scaffolds of polycaprolactone reinforced with in situ generated hydroxyapatite for bone tissue engineering. *J Mater Sci Mater Med.* 2010; 21(1): 343-351.
48. Ghaffari A, Navaee K, Oskoui M, Bayati K, Rafiee-Tehrani M. Preparation and characterization of free mixed-film of pectin/chitosan/Eudragit® RS intended for sigmoidal drug delivery. *Eur J Pharm Biopharm.* 2007; 67(1): 175-186.
49. Wan Y, Wu H, Yu A, Wen D. Biodegradable polylactide/chitosan blend membranes. *Biomacromolecules.* 2006; 7(4): 1362-1372.
50. Roohani-Esfahani S, Nouri-Khorasani S, Lu Z, Appleyard R, Zreiqat H. Effects of bioactive glass nanoparticles on the mechanical and biological behavior of composite coated scaffolds. *Acta Biomater.* 2011; 7(3): 1307-1318.
51. Bolaina-Lorenzo E, Martínez-Ramos C, Monleón-Pradas M, Herrera-Kao W, Cauich-Rodríguez JV, Cervantes-Uc JM. Electrospun polycaprolactone/chitosan scaffolds for nerve tissue engineering: physicochemical characterization and Schwann cell biocompatibility. *Biomed Mater.* 2016; 12(1): 015008.
52. Liu H, Liu W, Luo B, Wen W, Liu M, Wang X, Zhou C. Electrospun composite nanofiber membrane of poly (l-lactide) and surface grafted chitin whiskers: fabrication, mechanical properties and cytocompatibility. *Carbohydr Polym.* 2016; 147: 216-225.
53. Sailema-Palate GP, Vidaurre A, Campillo-Fernández A, Castilla-Cortázar I. A comparative study on Poly (ε-caprolactone) film degradation at extreme pH values. *Polym Degrad Stab.* 2016; 130: 118-125.
54. Bikiaris D, Panayiotou C. LDPE/starch blends compatibilized with PE-g-MA copolymers. *J Appl Polym Sci.* 1998; 70(8): 1503-1521.
55. Wu C-S. A comparison of the structure, thermal properties, and biodegradability of polycaprolactone/chitosan and acrylic acid grafted polycaprolactone/chitosan. *Polymer.* 2005; 46(1): 147-155.
56. Díaz E, Sandonis I, Valle MB. In vitro degradation of poly (caprolactone)/nHA composites. *J Nanomater.* 2014; 2014: 185-193.
57. Woodruff MA, Hutmacher DW. The return of a forgotten polymer—polycaprolactone in the 21st century. *Prog Polym Sci.* 2010; 35(10): 1217-1256.
58. Liu H, Leonas KK. Weight loss and morphology changes of electrospun poly (caprolactone) yarns during in vitro degradation. *FIBER POLYM.* 2010; 11(7): 1024-1031.
59. Heimowska A, Morawska M, Bocho-Janiszewska A. Biodegradation of poly (ε-caprolactone) in natural water environments. *Pol J Chem Technol.* 2017; 19(1): 120-126.
60. Thuaksuban N, Nuntanarant T, Pattanachot W, Suttapreyasri S, Cheung LK. Biodegradable polycaprolactone-chitosan three-dimensional scaffolds fabricated by melt stretching and multilayer deposition for bone tissue engineering: assessment of the physical properties and cellular response. *Biomed Mater.* 2011; 6(1): 015009.
61. Nithya R, Sundaram NM. Biodegradation and cytotoxicity of ciprofloxacin-loaded hydroxyapatite-polycaprolactone nanocomposite film for sustainable bone implants. *Int J Nanomedicine.* 2015; 10(Suppl 1):119-127.
62. Shao H-J, Lee Y-T, Chen C-S, Wang J-H, Young T-H. Modulation of gene expression and collagen production of anterior cruciate ligament cells through cell shape changes on polycaprolactone/chitosan blends. *Biomaterials.* 2010; 31(17): 4695-4705.
63. Hamilton V, Yuan Y, Rigney D, Puckett A, Ong J, Yang Y, Elder S, Bumgardner J. Characterization of chitosan films and effects on fibroblast cell attachment and proliferation. *J Mater Sci Mater Med.* 2006; 17(12): 1373-1381.
64. Chung T-W, Liu D-Z, Wang S-Y, Wang S-S. Enhancement of the growth of human endothelial cells by surface roughness at nanometer scale. *Biomaterials.* 2003; 24(25): 4655-4661.
65. Rezwan K, Chen Q, Blaker J, Boccaccini AR. Biodegradable and bioactive porous polymer/inorganic composite scaffolds for bone tissue engineering. *Biomaterials.* 2006; 27(18): 3413-3431.
66. Ghasemi-Mobarakeh L, Prabhakaran MP, Morshed M, Nasr-Esfahani M-H, Ramakrishna S. Electrospun poly (-caprolactone)/gelatin nanofibrous scaffolds for nerve tissue engineering. *Biomaterials.* 2008; 29(34): 4532-4539.